TECHNICAL REPORT

SPACE TELESCOPE SCIENCE INSTITUTE
Operated for NASA by AURA

Title: Mid-InfraRed Instrument (MIRI) Target Acquisition Strategies and Use Cases		Doc #: JWST-STScI-001407, SM-12 Date: May 28, 2008 Rev: -
Authors: Karl Gordon & Margeret Meixner	Phone: 410-331-5031	Release Date: 2 June 2008

1.0 Abstract

Target acquisition will be required for the Mid-Infrared Instrument (MIRI) on JWST for medium resolution spectroscopy with the integral field unit (MRS-IFU), low-resolution spectroscopy with a slit (LRS-Slit), coronagraphy with the Lyot phase mask, and coronagraphy with the 4-quadrant phase masks (4QPM). The target acquisition steps for each of these 4 modes of observations with MIRI are given. Target acquisition is allowed in 4 filters (F560W, F1000W, F1500W, and neutral density) and exposures up to 990 MIRI seconds are possible to allow for target acquisition on faint sources.

2.0 Introduction

Target acquisition uses images from a JWST science instrument to determine corrections that improve the precision of pointed observations over the usual pointing obtained with the fine guidance sensors. MIRI has three observing types with small apertures or masks that necessitate target acquisition: medium resolution spectroscopy with the integral field unit (MRS-IFU), low-resolution spectroscopy with a slit (LRS-Slit), coronagraphy with the Lyot phase mask, and coronagraphy with the 4-quadrant phase masks (4QPM). In this memo, we outline use cases for the target acquisition for these four observing types.

It is assumed that the MIRI is in a configuration that protects against saturation latents. In other words, something like the filter wheel has been rotated to put the ND filter or prism in the beam.

2.1 Definitions

In this document:

frames (= reads in Spitzer terminology)

MIRI second = 0.92 real seconds

2.2 Filters

The filter used for the target acquisition can be the neutral density filter or one of 4 broadband filters. The broadband filters possible are F560W, F1000W, and F1500W that were chosen to span the range of MIRI wavelengths while at the same time allow for centroiding accuracies of 5-20 mas to be achieved. Simulations (see section 2.4) have shown that it is not possible to measure a centroid to 20 mas with the F2550W filter for a source of any brightness. The choice of which filter to use should be determined by the proposer based on the type of source for target acquisition.

2.3 Subarray size

The goal of the target acquisition subarrays will be to use the smallest region possible limited by the accuracy of the guide star acquisition positional uncertainty. It is likely that a 32x32 pixel subarray will be the nominal size for all MIRI target acquisitions, but it may be necessary to change the size of the subarray based on the on orbit capabilities of the JWST pointing. Each group used is taken as a full frame, but only the subarray region is stored onboard to be used in the target acquisition algorithm.

2.4 Subarray slope image creation

For bright stars, the standard method for creating the slope image can be used. This involves using either 4 FASTMode or 4 SLOWMode groups to create 2 estimates of the slope and using the minimum of the two estimates as the slope value for each pixel.

For fainter stars where longer than the shortest integration times are needed, the "enhanced standard" method (Gordon et al. 2008) should be used. This method consists of taking an integration with 4n + 1 groups. Due to data volume constraints, the SLOWMode integrations with 4n + 1 groups will be taken using a 512x512 subarray with 4 frames coadded per group. This results in the same group time as a full frame group, but with ¼ the data volume. The first group is rejected and the resulting 4 subexposures are used to create 4 slope estimates. These slope estimates are calculated by subtracting the last group from the first group in each subexposure. The minimum of the 4 slope estimates is taken and this will remove up to 3 cosmic rays (a long exposure may have multiple cosmic rays in a single pixel). The number of groups needed for faint sources should be determined by the ground system from the user input source flux.

Table 1: Readout mode and Slope Creation Method

Exptime	Readout Mode	# groups	Slope Creation Method
<= 12 MIRI sec	FASTMode	4	Standard
<= 120 MIRI sec	SLOWMode	4	Standard
> 120 MIRI sec	SLOWMode	4n + 1	Enhanced Standard

Eq. 1: $\text{Exptime} = A(\text{Flux})^B$

Where A & B are from Table 2, and Flux is in units of microJy. The allowed exposure times are 12, 120, 270, 390, 510, 630, 750, 870, and 990 MIRI seconds. The coefficients were determined using simulations of the centroiding accuracy as described in Gordon et al. (2008). As an example of this process, the set of runs used to determine the coefficients for the F560W filter is shown in Figure 1.

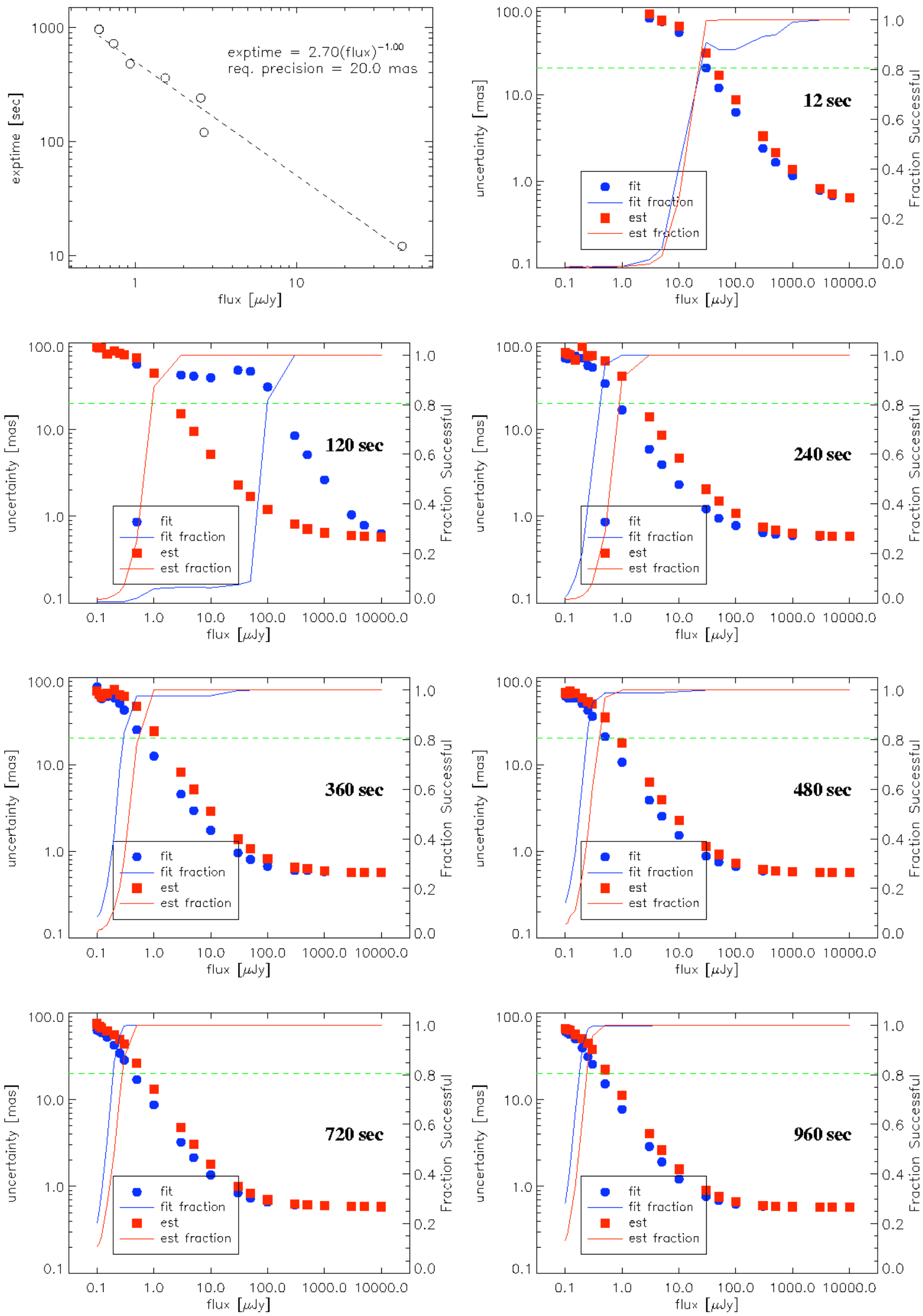

Figure 1: Example results for simulations to determine the exposure time for the F560W filter for a centroiding accuracy of 20 mas (green dashed line). The red squares were used to determine the flux which 20 mas is possible, and the resulting fit versus flux is shown in the top left plot. The blue circles are the results using a least squares linear fit. The least squares fit fails for 120 MIRI sec as

there are only 4 frames and it is not possible to remove cosmic rays before the linear fit with this few samples. In the plots, sec = MIRI seconds. For more details on the simulations and plots see Gordon et al. (2008).

2.5 Slope Image Processing

The slope image should be flat fielded using the stored flat field specific for each subarray region used. This stored flat field is generated on the ground and uploaded to JWST. It will be stored as a 16bit integer array to save space. The easiest way to do this is to scale the flat field by slightly more than the maximum value in the subarray region such that all of the numbers are less than 1. The overall level of the flat field is not important, just that the variations from pixel-to-pixel are removed. The resulting floating point numbers can then be converted to integers (e.g., 0.967 -> 967). The onboard algorithm will make the appropriate conversion before the flat field division step.

It may be necessary to mask some bad pixels (e.g., hot or dead). This would be required if no clean region without bad pixels can be found in the appropriate area of the detector or, later in the mission, when damage may have accumulated such that the density of bad pixels is much higher. In this case, the values of the bad pixels should be replaced by an average of the neighboring pixels.

The background should be subtracted from the slope image before being input into the floating centroid algorithm. Nominally, the background should be determined in the standard method that is to pick the pixel that is 30% from the minimum. It may be possible to simplify this step, but further simulations are necessary to determine if simpler background subtraction options are viable.

2.6 Centroiding algorithm

For all the modes, the basics of the target location (centroiding) are the same. A varying number of groups are processed to produce a slope image that is free of cosmic rays. The floating centroid method (Meixner et al. 2007) should be used for determining the location of the source. The iteration threshold (tolerance error) is 0.01. The maximum number of iterations is 15. Both of these numbers were taken as defaults from the find_varwindow_moment.pro program (Meixner et al. 2007). The optimal values may be different. The size of the checkbox (used for finding the initial peak in the subarray region) and the centroidbox (used for the floating centroid algorithm itself) are 2 and 5 pixels, respectively.

3.0 Medium Resolution Spectroscopy – Integral Field Unit (MRS-IFU)

The goal is to take a spectrum of a source. The required accuracy of placing a source in the field of view of the IFU is 90 mas (milliarcsec) (Glasse 2006). This accuracy is ½ the slice width at the shortest wavelength. This required accuracy limits the spacecraft move between the target acquisition region and the center of the IFU to be less than 50" (Sivaramakrishnan et al. 2006). The centroid accuracy necessary not to significantly affect the accuracy is 20 mas.

3.1 Point Sources

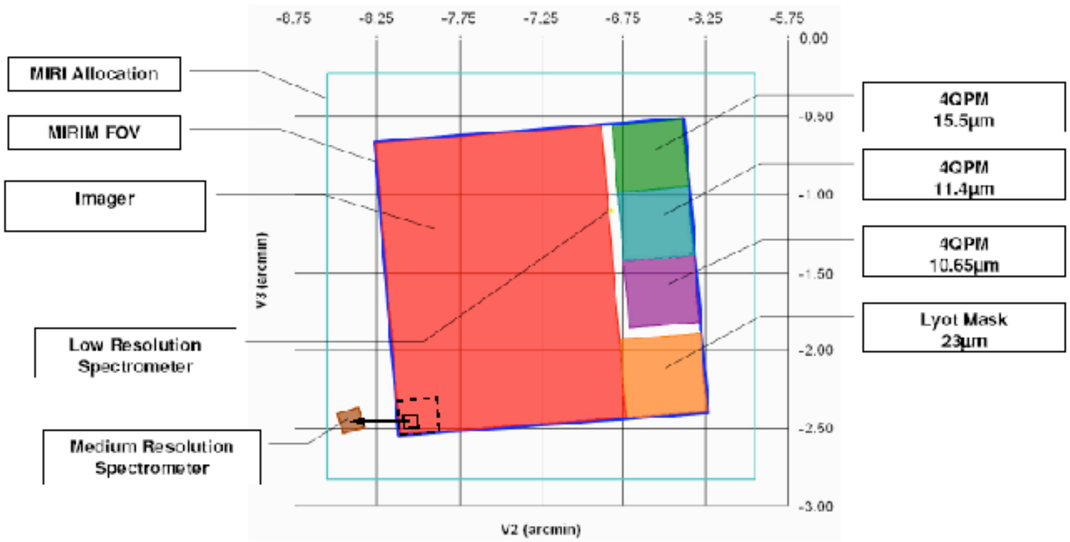

Figure 2: The MIRI field of view is shown. The large dashed box in the red imager region is the region in which the MRS-IFU target acquisition region should be located and the small solid box is the approximate proposed location. The required spacecraft offset is shown as an arrow.

The point source is placed on the part of the imager field of view closest to the IFU field of view. This is illustrated in Figure 2. The dashed region shows the region where the target acquisition subarray should be located; roughly between (896,896) and (1024,1024) in pixel coordinates. While the final target acquisition location will need to be determined on orbit to avoid any hot or dead pixels, the region should be centered on pixel coordinates (950,950). The choice of the readout mode and slope creation method can be determined from the required exposure time using **Error! Reference source not found.**. The exposure time can be determined from Eq. 1 and the coefficients in Table 2. The minimum flux for which centroiding is possible at the required accuracy is given for 12 and 990 MIRI seconds in Table 2.

The target acquisition sequence would be:

1. Command the spacecraft to move the source to center of the MRS-IFU target acquisition subarray region
2. Rotate the filter wheel to the proposer selected filter
3. **Bright sources**: Take 4 full groups in FASTMode or SLOWMode
4. **Faint sources**: Take 4n+1 full groups in SLOWMode
5. Extract the subarray region
6. **Bright sources**: Create the slope image using the "standard" method
7. **Faint sources**: Create the slope image using the "enhanced standard" method
8. Flat field image using stored flat field specific for this subarray region
9. Subtract the background
10. Perform the floating centroid algorithm to determine source location
11. Compute the spacecraft offset needed to place the source at the 1st dither position relative to the center of the smallest IFU (3.5"x3.5").

12. The nominal offset is approximately (30", 0) in (V2, V3).
13. Command the spacecraft move
14. Start taking MRS-IFU data

Table 2: Coefficients (Eq. 1) for MRS-IFU for each filter

Coefficients	ND	F560W	F1000W	F1500W
A	5.87	2.70	3.70	5.32
B	-0.90	-1.00	-1.21	-1.49
Flux(12 MIRI sec) [μJy]	2.4×10^5	45	150	710
Flux(990 MIRI sec) [μJy]	2200	0.60	4.0	38

3.2 Offset from Nearby Point Source

A bright nearby point source can be used instead of the target source. The only restriction is that the offset source position does not require a greater than 50" spacecraft move to put the target source into the IFU. The target acquisition sequence given in section 3.1 is then used, modulo the need to compute the spacecraft move taking into account the relative positions of the offset source and the target source.

It may be acceptable to use an offset source that requires a greater than 50" spacecraft move and accept a larger uncertainty in the target position than the requirements. This would allow for sources with very uncertain positions to be placed in the IFU field-of-view with better than the uncertainties produced by the JWST blind pointing as long as there is an offset source with a well measured position. There is a limit of approximately 60" on the largest spacecraft move that can be done while using the same guide star. Thus, the relaxation of the use of an offset source is only to something like 60" from 50". Not a major increase in the number of allowed offset stars.

3.3 No Target Acquisition

There will be observations with the MRS-IFU that do not require target acquisition. Examples of such observations are spectral mapping of regions or measurements faint diffuse regions where precise pointing is not necessary.

4.0 Low Resolution Spectroscopy – Slit (LRS-Slit)

The goal is to take a spectrum of a source. The required accuracy of placing a source in the slit is 20 mas (milliarcsec) (Glasse 2006). This accuracy is set to allow for the required wavelength accuracy to be achieved. The LRS slit is 5.5"x0.6". This required accuracy limits the spacecraft move between the target acquisition region and the center of the IFU to be less than 20" (Sivaramakrishnan et al. 2006). The centroid accuracy necessary not to significantly affect the required target acquisition accuracy is 5 mas.

4.1 Point Sources

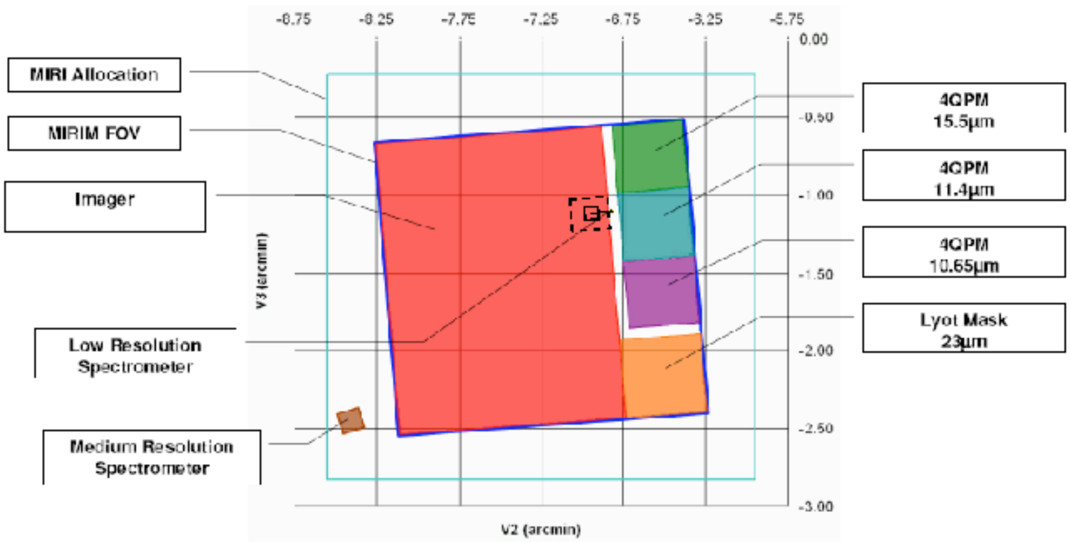

Figure 3: The MIRI field of view is shown. The large dashed box in the red imager region is the region in which the LRS-Slit target acquisition region should be located and the small solid box is the approximate proposed location. The required spacecraft offset is shown as an arrow.

The point source is placed on the part of the imager field of view closest to the LRS slit. This is illustrated in Figure 3. The dashed region shows the region where the target acquisition subarray should be located; roughly between (320,256) and (448,384) in pixel coordinates. While the final target acquisition location will need to be determined on orbit to avoid any hot or dead pixels, the region should be centered on pixel coordinates (384,320). The choice of the readout mode and slope creation method can be determined from the required exposure time using **Error! Reference source not found.**. The exposure time can be determined from Eq. 1 and the coefficients in Table 3. The minimum flux for which centroiding is possible at the required accuracy is given for 12 and 990 MIRI seconds in Table 3.

The target acquisition sequence would be:

1. Command the spacecraft to move the source to center of the MRS-IFU target acquisition subarray region
2. Rotate the filter wheel to the proposer selected filter
3. **Bright sources**: Take 4 full groups in FASTMode or SLOWMode
4. **Faint sources**: Take 4n+1 full groups in SLOWMode
5. Extract the subarray region
6. **Bright sources**: Create the slope image using the "standard" method
7. **Faint sources**: Create the slope image using the "enhanced standard" method
8. Flat field image using stored flat field specific for this subarray region
9. Subtract the background
10. Perform the floating centroid algorithm to determine source location
11. Compute the spacecraft offset needed to place the source at the 1st dither position relative to the center of the slit.

12. The nominal offset is approximately 10.5” (96 pixels) in the x pixel direction.
13. Command the spacecraft move
14. Start taking LRS-Slit data

Table 3: Coefficients (Eq. 1) for LRS-Slit for each filter

Coefficients	ND	F560W	F1000W	F1500W
A	6.98	3.28	4.65	6.17
B	-0.92	-0.95	-1.25	-1.28
Flux(12 MIRI sec) [μJy]	2.6×10^6	237	750	8300
Flux(990 MIRI sec) [μJy]	23000	2.7	25	290

4.2 Offset from Nearby Point Source

It may be acceptable to use an offset source that requires a greater than 20” spacecraft move and accept a larger uncertainty in the target position than the requirements. This would allow for sources with very uncertain positions to be placed in the LRS slit field-of-view with better than the uncertainties produced by the JWST blind pointing as long as there is an offset source with a well measured position There is a limit of approximately 60” on the largest spacecraft move that can be done while using the same guide star. Thus, the relaxation of the use of an offset source is only to something like 60” from 20”. This is a major increase in the number of allowed offset stars.

4.3 No Target Acquisition

There will be observations with the LRS-Slit that do not require target acquisition. Examples of such observations are spectral mapping of regions or measurements faint diffuse regions where precise pointing is not necessary.

5.0 Coronagraphy – Lyot

The goal is to take a coronagraphic image of a source to search for nearby sources and or structures. The required accuracy of placing a source in the slit is 22.5 mas (milliarcsec) (the accuracy requirement is desired for high quality science, but is not a formal requirement). This accuracy is set to achieve the best cancellation of the central point source. This required accuracy limits the spacecraft move between the target acquisition region and the center of the Lyot spot to be less than 20” (Sivaramakrishnan et al. 2006). The centroid accuracy necessary not to significantly affect the required target acquisition accuracy is 5 mas.

5.1 Point Sources

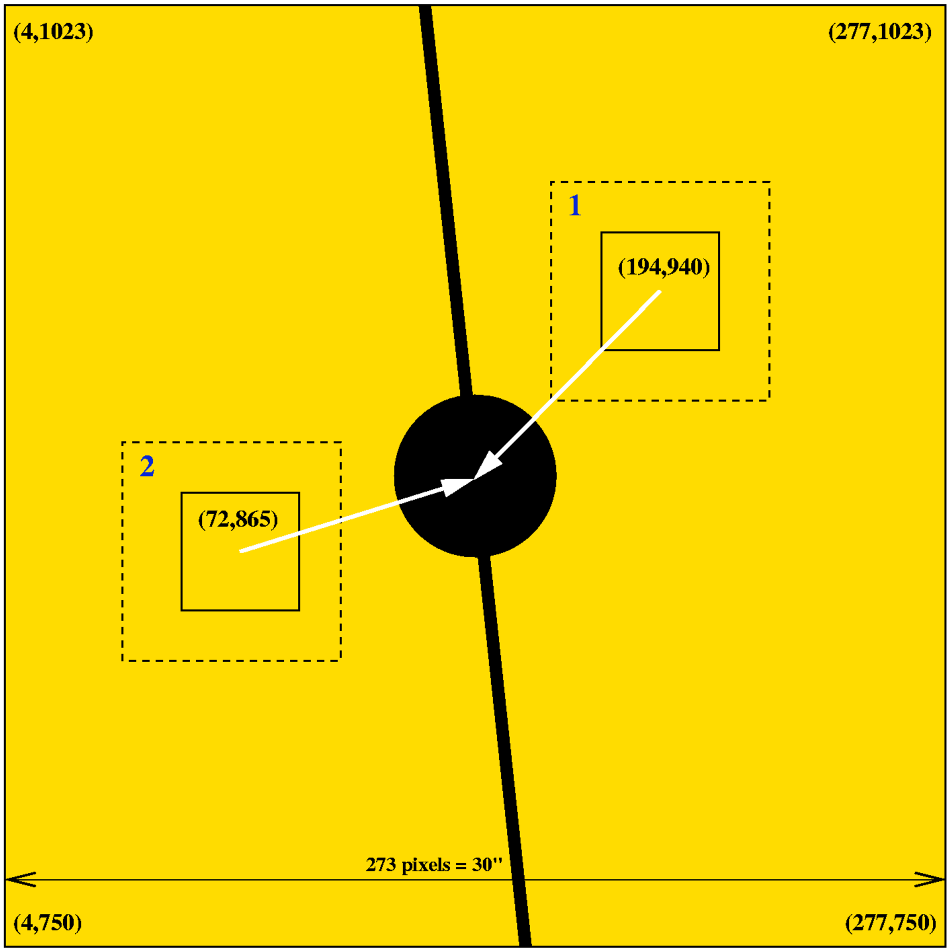

Figure 4: The MIRI Lyot coronagraphy field-of-view is shown. The large dashed boxes are the regions in which the Coronagraphy-Lyot target acquisition region should be located and the small solid boxes are the approximate proposed locations. The required spacecraft offsets are shown as an arrow.

The point source is placed in one of the two target acquisition subarray regions in the Lyot coronagraphic field of view. For Lyot coronagraphy, there is a specific readout subarray defined which encompasses the entire Lyot coronagraphic region (MASKLYOT, 320x320 pixels). The readout times for this subarray in FASTMode and SLOWMode are 0.274 seconds and 2.74 seconds, respectively (Gordon & Meixner 2008). The two regions are illustrated in Figure 4. The dashed regions show the 64x64 pixel regions where the target acquisition subarrays should be located. There are two target acquisition subarrays needed. Given the brightness of the sources, it is possible that the target acquisition will leave a latent image in the target acquisition region. To mitigate confusing the latent image with a nearby faint source, it will be optimal to take two coronagraphic observations: one with target acquisition using the 1st subarray region and one with target acquisition using the 2nd subarray region. The saturation latents will be different between the two coronagraphic observations allowing for discrimination of faint sources and saturation latents. The discrimination is possible as the observations taken with the 1st target acquisition region will not have latents in the 2nd target acquisition region and the latents are variable in time such that the latents in the 1st subarray region will have decayed by the time the 2nd subarray region target acquisition observations are done. The locations of the subarrays are given in Table 4. The goal is these regions should be located as close to the center of the Lyot spot (radius = 2.4"; Renouf 2006) as possible without being affected by any edge effects. The accuracy of spacecraft small angle maneuvers from 2"-20" is 20 mas (Sivaramakrishnan et al. 2006).

Table 4: Centers and nominal offsets (pixels) of Lyot target acquisition subarrays

Subarray	Size	Location	Nominal offset
1	32x32	(194,940)	1-center, (-53,-53)
2	32x32	(72,865)	2-center, (68,22)

The choice of the readout mode and slope creation method can be determined from the required exposure time using Table 5. The exposure time can be determined from Eq. 1 and the coefficients in Table 6. The minimum flux for which centroiding is possible at the required accuracy is given for 1.096 and 90.42 seconds in Table 6.

Table 5: Readout mode and Slope Creation Method for Lyot readout subarray

Exptime	Readout Mode	# groups	Slope Creation Method
<= 1.096 sec	FASTMode	4	Standard
<= 10.96 sec	SLOWMode	4	Standard
> 10.96 sec	SLOWMode	4n + 1	Enhanced Standard

The target acquisition sequence would be:

1. Command the spacecraft to move the source to center of the 1st Coronagraphy-Lyot target acquisition subarray region
2. Rotate the filter wheel to the proposer selected filter (likely the ND filter)
3. **Bright sources**: Take 4 readout subarray groups in FASTMode or SLOWMode
4. **Faint sources**: Take 4n+1 readout subarray groups in SLOWMode
5. Close the CCC to prevent saturation latents when moving and changing filters
6. Extract the target acquisition subarray region from the readout subarray groups
7. **Bright sources**: Create the slope image using the "standard" method
8. **Faint sources**: Create the slope image using the "enhanced standard" method
9. Flat field image using stored flat field specific for this subarray region
10. Subtract the background
11. Perform the floating centroid algorithm to determine source location
12. Compute the spacecraft offset needed to place the source at the center of the Lyot spot.
13. The nominal offset is approximately 8" (73 pixels).
14. Command the spacecraft move

15. Rotate the filter wheel to the F2300C filter
16. Open the CCC
17. Start taking Coronagraphy-Lyot data
18. Repeat steps 1-16 using the 2nd Coronagraphy-Lyot target acquisition subarray region

Table 6: Coefficients (Eq. 1) for Coronagraphy-Lyot for each filter

Coefficients	ND	F560W	F1000W	F1500W
A	6.42	2.73	4.26	5.79
B	-0.92	-0.95	-1.25	-1.28
Flux(1.096 sec) [μJy]	$8.3x10^6$	783	2500	27000
Flux(90.42 sec) [μJy]	76000	9.0	82	950

6.0 Coronagraphy – 4-quadrant phase masks

The goal is to take a coronagraphic image of a source to search for nearby sources and or structures. The required accuracy of placing a source in the slit is 5 mas (the accuracy requirement is desired for high quality science, but is not a formal requirement). This accuracy is set to achieve the best cancellation of the central point source given that there is no coronagraphic spot for the 4QPM mode. This accuracy limits the spacecraft move between the final target acquisition region and the center of the 4-quadrant phase mask to be less than 0.5" (Sivaramakrishnan et al. 2006).

6.1 Point Sources

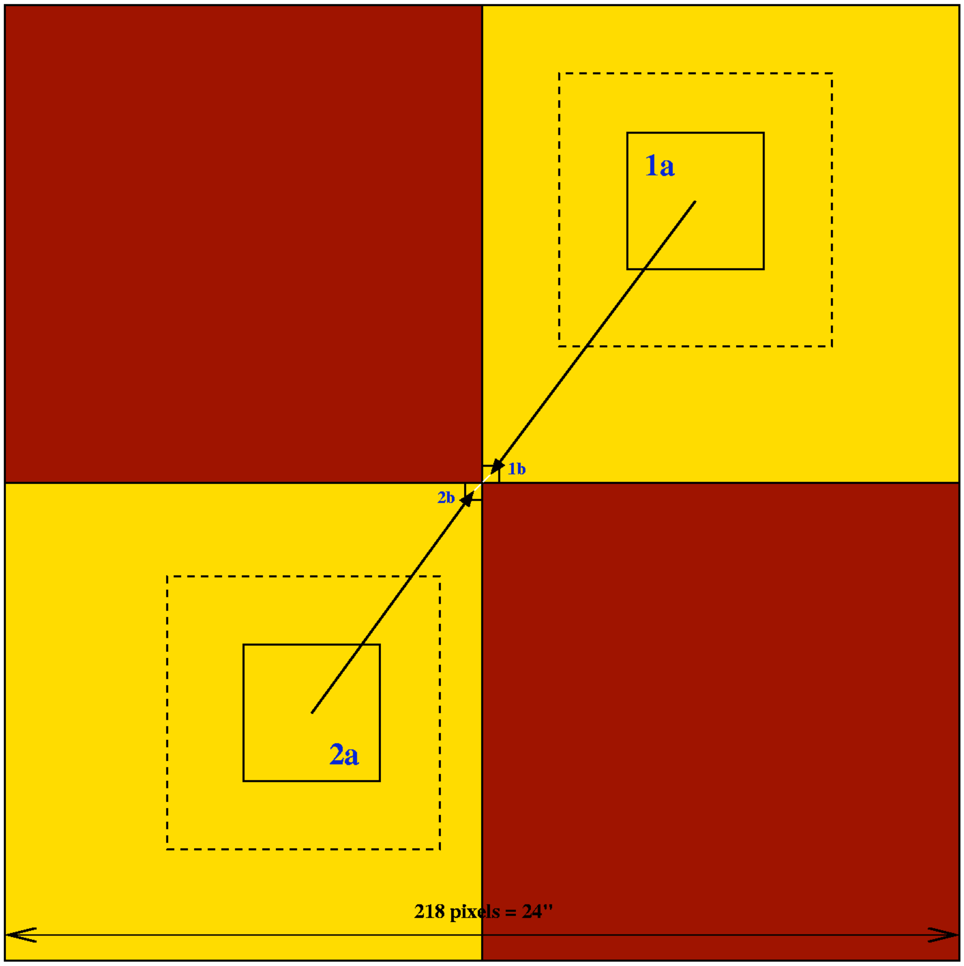

Figure 5: One of the MIRI 4-quadrant phase mask coronagraphy field-of-views is shown. The large dashed boxes are the regions in which the "a" Coronagraphy-4QPM target acquisition region should be located and the small solid boxes are the approximate proposed locations. The required spacecraft offsets are shown using arrows.

The coronagraphic 4-quadrant phase mask target acquisition requires a two-step process. First, a target acquisition region approximately in the center of one of the four quadrants is used to locate the target. Then a spacecraft move is used to place the source in a second target acquisition region very near (<0.5") the center of the coronagraphic field-of-view. The target is located again and then moved using the most precise small spacecraft moved into the center of the coronagraphic field-of-view. For 4QPM coronagraphy, there are specific readout subarrays defined which encompasses the entire 4QPM coronagraphic regions (MASK1550, MASK1140, & MASK1065; all 256x256 pixels). The readout times for this subarray in FASTMode and SLOWMode are 0.179 seconds and 1.79 seconds, respectively (Gordon & Meixner 2008). This is illustrated in Figure 5. Due to saturation latents, this procedure has to be done twice where the direction the center if approached is different by approximately 180 degrees. The saturation latents will be different between the two coronagraphic observations allowing for discrimination of faint sources and saturation latents. The discrimination is possible as the observations taken with the 1st target acquisition regions (1a & 1b) will not have latents in the 2nd target acquisition regions (2a & 2b) and the latents are variable in time such that the latents in the 1st subarray regions will have decayed by the time the 2nd subarray regions target acquisition observations are done. The locations of the subarrays on each of the three 4-quadrant phase masks are given in Table 7. The "a" subarrays are 32x32 pixels and the "b" subarrays are 4x4 pixels. The uncertainty in the position of the source in the "b" subarrays is approximately 20 mas (8" spacecraft move from "a" to "b" subarrays). Thus, the sizes of the "b" subarrays (0.44"x0.44") are large enough so the source will always be in it the same pixel in the "b" subarray regions after the "a" target acquisition.

Table 7: Centers and nominal offsets (pixels) of 4-quadrant phase mask target acquisition subarrays

Subarray	Size	10.65 μm	11.4 μm	15.5 μm	Nominal offset
1a	32x32	(163,625)	(163,402)	(163,174)	1a-1b, (-50, -64)
1b	4x4	(115,562)	(115,340)	(115,112)	1b-center, (-2,-2)
2a	32x32	(74,508)	(74,285)	(74,57)	2a-2b, (40,53)
2b	4x4	(111,559)	(111,336)	(111,108)	2b-ceneter (2,2)

The choice of the readout mode and slope creation method can be determined from the required exposure time using Table 8. The exposure time can be determined from Eq. 1 and the coefficients in Table 9. The minimum flux for which centroiding is possible at the required accuracy is given for 0.716 and 59.07 seconds in Table 9.

Table 8: Readout mode and Slope Creation Method for Lyot readout subarray

Exptime	Readout Mode	# groups	Slope Creation Method
<= 0.716 sec	FASTMode	4	Standard
<= 7.16 sec	SLOWMode	4	Standard
> 7.16 sec	SLOWMode	4n + 1	Enhanced Standard

The target acquisition sequence would be:

1. Command the spacecraft to move the source to center of the 1a (or 2a for 2nd pass) target acquisition subarray region
2. Rotate the filter wheel to the proposer selected filter (likely the ND filter)
3. **Bright sources**: Take 4 readout subarray groups in FASTMode or SLOWMode
4. **Faint sources**: Take 4n+1 readout subarray groups in SLOWMode
5. Close the CCC to prevent saturation latents when moving and changing filters
6. Extract the subarray region
7. **Bright sources**: Create the slope image using the "standard" method

8. **Faint sources**: Create the slope image using the "enhanced standard" method
9. Flat field image using stored flat field specific for this subarray region
10. Subtract the background
11. Perform the floating centroid algorithm to determine source location
12. Compute the spacecraft offset needed to place the source in the center of the "b" region.
13. The nominal offsets are given in Table 4.
14. Command the spacecraft move
15. Open the CCC
16. Repeat steps 3-10.
17. Compute the spacecraft offset needed to place the source in the center of the coronagraphic field-of-view.
18. [TBD] Steps 14-16 may be repeated n times to improve the acquisition (see Section 6.2)
19. The nominal offsets are given in Table 4.
20. Command the spacecraft move
21. Rotate the filter wheel to the appropriate filter for the coronagraph being used (i.e., F1065C, F1140C, or F1550C)
22. Open the CCC
23. Start taking Coronagraphy-4QPM data
24. Repeat steps 1-24 using the 2nd Coronagraphy-4QPM target acquisition subarray region

Table 9: Coefficients (Eq. 1) for Coronagraphy-4QPM for each filter

Coefficients	ND	F560W	F1000W	F1500W
A	6.32	2.63	4.19	5.73
B	-0.92	-0.95	-1.25	-1.28
Flux(0.716 sec) [μJy]	$1.0x10^7$	970	3100	34000
Flux(59.07 sec) [μJy]	94000	11	100	1200

6.2 Possible Iterative Target Acquisition

It may be possible to improve the 4QPM target acquisition accuracy by repeatedly performing the centroiding algorithm and spacecraft moves in the central position. If there is no or minimal distortion of the point spread function due to the intersection of the 4 glass plates making up the 4QPM when the source is in the center of the 4QPM, then it should be possible to improve the target acquisition beyond the nominal 1-sigma 5 mas in each axis given by the spacecraft move (< 0.5") error. This will be tested at the beginning of the mission to determine if it is possible.

This iterative method would involve moving the pixel centers of the 1b and 2b regions to the center of the subarray region, making them the same region. Then the centroiding and spacecraft move actions (steps 14-16 in section 6.1) would be repeated up to n times.

The number of times (n) to repeat steps 14-16 and if there is a criteria to stop repeating before reaching n would be determined on orbit. There are two proposed methods.

The first is to repeat steps 14-16 until the centroid determined is within some absolute accuracy requirement (e.g., 5 mas on each axis) up to some maximum allowed number of repeats. The details of this strategy can be found in Cavarroc et al. (2008). The main idea is that at some point, the source will fall into the central position with an accuracy better than is achieved on average with a single move.

The second is to repeat steps 14-16 a deterministic number of times. The idea is that once the source is in the central position, the accuracy of a very small spacecraft move and the ability to determine the required move may be significantly better. The required move would be less than a pixel and this means the centroid measurements and move repeats would be done in the same pixel.

Achieving 5 mas absolute accuracy with the target acquisition will be challenging this will be pushing for the best possible accuracy and may not be achievable. It is likely that there may be issues that may limit the accuracy possible to larger than 5 mas. The true amplitude of these issues will only be known after launch. These issues include:

1. Random spacecraft jitter (7 mas)
2. Knowledge of the angle between the FGS and MIRI FOV (1 arcsec uncertainty -> 5 mas?)
3. Smallest spacecraft move possible (1 mas?)
4. Nature of the uncertainties on spacecraft moves (random or biased)

7.0 Conclusions

The detailed steps are listed to perform target acquisition for the MIRI MRS-IFU, LRS-Slit, coronagraphy-Lyot, and coronagraphy-4QPM. The required target acquisition accuracies are possible for all the modes, with the exception of coronagraphy-4QPM where only on orbit will it be possible to determine if the stringent requirements can be met. Target acquisition is possible in 4 filters (F560W, F1000W, F1500W, and neutral density) and for exposure times up to 990 MIRI seconds (MRS-IFU & LRS-Slit), 90.42 seconds (coronagraphy-Lyot), and 59.07 seconds (coronagraphy-4QPM). Simulations were used to determine the exposure times in each mode to achieve the required accuracy given an input source flux and target acquisition filter choice.

8.0 Contributors to memo:

Celine Cavarroc, Anthony Boccaletti, Ed Nelan, Vicki Balzano, George Rieke, and entire MIRI Team

9.0 References

Sivaramakrishnan, A. et al. 2006, NGST, DRD#D36177, Rev. B, "JWST Pointing Error Allocation and Performance Prediction Analysis,"

Cavarroc, C. et al. 2008, MIRI-TN-0619-CEA, "Coronography Target Acquisition Strategy"

Glasse, A. 2006, MIRI-RP-00027-ATC, "The MIRI Calibration Error Budget"

Gordon, K. et al., 2008, JWST-STScI-001347, "MIRI (Mid-Infrared Instrument) Low Resolution Target Acquisition for Faint Sources"

Meixner, M., Cavarroc, C., Regan, M., & Boccaletti, A., 2007, JWST-STScI-001134, "Target Location Algorithms for the Mid-Infrared Instrument (MIRI)"

Meixner, M. & Gordon, K. JWST-STScI-000910, "Mid-Infrared Instrument (MIRI) Operations Concept Document JPL D-25632"

Renouf, I. 2006, MIRI-DD-00001-AEU "Mid-Infrared Instrument (MIRI) OBA Design Description DRL SI-01"